Mecánica Computacional Vol. XXIII, pp. 2979-2998
G.Buscaglia, E.Dari, O.Zamonsky (Eds.)
Bariloche, Argentina, November 2004

ELLIPTIC PROBLEMS WITH ESSENTIAL BORDER SINGULARITIES: IMPROVED SOLUTION AND QUALITATIVE ERROR ESTIMATION

Marta B. Bergallo*, **Carlos E. Neuman***, **and Victorio V. Sonzogni†**

*Grupo de Análisis Numérico(DM), Facultad de Ingeniería Química
Universidad Nacional del Litoral
Santiago del Estero 2829, 3000 Santa Fe, Argentina
e-mail: mbergallo@fiqus.unl.edu.ar,ceneuman@fiqus.unl.edu.ar

†Centro Internacional de Mecánica Computacional CIMEC, INTEC, UNL, CONICET
Gemes 3450, 3000 Santa Fe, Argentina
e-mail: sonzogni@intec.unl.edu.ar

Key Words: Mixed meshes, Elliptic problems, Border singularities, *A posteriori* errors

Abstract. *In the last twenty years two demanding problems were concurrently studied by the chemical engineering and mathematical researchers: the modelling of chemical reactors and other similar devices and the processes inside them and the numerical (and analytical) solutions of the sets of differential algebraic equations that these models provide them. In this paper a complex subproblem of those just described is considered: the appearance of singularities in the domain or the border of the modelled process device in the case of PDE models.*

The idea of this work is to isolate the possible singularities by means of simplifying the phenomenological models as far as possible and assessing the errors in the numerical solutions using classical methods and, in particular, the mixed mesh qualitative error estimation method proposed by the authors. The main idea of this mixed or composite mesh method is to construct a numerical model where two or more finite element meshes of different granularities are superimposed over the whole domain of the problem.

The mentioned simplifications produce several 1D and 2D differential equation problems with singularities in the domain and in its border that are solved and their errors studied.

The main conclusion of this presentation is the following: for the models the authors deal with it is possible to numerically detect the singularities and to devise computationally cheaper methods for their solution.

1 INTRODUCTION

In recent articles we have developed composite finite element models of several problems that are drawn from Mechanical and Chemical Engineering with the aim of providing reasonable *a posteriori* error estimates, and to obtain improved numerical solutions[1 2 3 4]. The main idea of this composite mesh method is to construct a numerical model where two or more finite element meshes of different granularities (size of the elements) are superimposed over the whole domain of the problem. The motivation of these developments came from the mixture theory of multiphase materials[5 6]. In this class of materials each component occupies a fraction of the total volume. The physical properties of the composite material is obtained from those of component phases weighted by a participation factor, which is taken as their volumetric fraction or another suitable quantity. In a similar way our numerical model is composed by different finite element meshes and the properties of the whole model is obtained by adding those of the component meshes multiplied by a participation factor. In this case, the different behavior of each component come from their intrinsic accuracy instead of their physical properties. In this work we study several properties associated to the application of the method to elliptic problems with boundary conditions of Dirichlet, Neumann, and mixed types and showing boundary singularities.

The finite element error estimates may be computed *a priori* or *a posteriori*. *A posteriori* error estimates, computed from the numerical solution, are of practical importance and may be categorized under two main subclasses. The first of these is stress recovery, which is also referred to as a postprocessing or flux-projection technique. It was proposed in the context of linear elliptic problems[7]. The second subclass are those of *residual based* estimators, explicit or implicit. The literature covering these topics is vast[8 9]. The error estimates performed by means of the composite mesh fall within the residual based estimators. The composite mesh, proposed in previous papers from the authors, is formed by two finite element meshes sharing the problem domain. The meshes have different element size h, and the connection between components is enforced, for instance, by connecting common nodes. The participation factors are defined as α and $(1-\alpha)$ for the fine and coarse meshes, respectively.

Several illustrating examples are treated in this paper:

1. The test problems based on variants of the elliptic stationary form of the heat equation

$$d\ u_t - \nabla \cdot (c \nabla u) + au = f \tag{1}$$

   with initial values, and boundary conditions of Dirichlet, Neumann and Robin type.

2. The elliptic stationary equation associated to the parabolic advection-diffusion equation

$$u_t - \Delta u + v \nabla u + p(u) = 0 \tag{2}$$

   with initial values, and boundary conditions of Dirichlet, Neumann and Robin type. In this equation p is a polynomial function.

3. Plane stress and strain problems drawn from linear elasticity.

A finite element model of the variational equation is then set, in order to discretize the problem in the space coordinates. The task is done in a mixed mesh framework designed to make *a posteriori* error estimation of the numerical solutions and to refine the mesh by means of an adaptive algorithm. The primary goal of the adaptive composite mesh finite element method for the stationary problem is to control the space discretization error of the approximate solution as measured from integrals of double mesh residuals. The adaptive process is of the h and of the h-r type.

The rest of the paper is devoted to the statement of some conclusions about the implementation details of the proposed method.

2 NOTATION, MODELS AND METHODS

The test problems we deal with are based on variants of the elliptic stationary form of the heat equation

$$-\nabla \cdot (c\nabla u) + au = f \tag{3}$$

with boundary conditions of Dirichlet ($hu = r$ on $\partial\Omega$), Neumann ($\eta \cdot (c\nabla u) = g$ on $\partial\Omega$) and Robin ($\eta \cdot (c\nabla u) + qu = g$ on $\partial\Omega$) type, where η is the outward unit normal, and g, q, h, and r are functions defined on $\partial\Omega$. Both, the linear and nonlinear cases are treated.

By standard calculations we derive the weak form of the differential equation: Find u such that

$$\int_{\Omega} ((c\nabla u) \cdot \nabla v + auv - fv)\, dx = \int_{\partial\Omega} (-qu + g)v\, ds, \;\; \forall v \tag{4}$$

The stationary elliptic counterpart of the diffusive-advective nonlinear equation case is also treated. The main equation is

$$-\nabla \cdot (c\nabla u) + v\nabla u + p(u) = 0 \text{ in } \Omega \tag{5}$$

where $p(u)$ is a polynomial function in u, with Dirichlet and Robin ($\eta \cdot (c\nabla u) + q(u) = 0$ on $\partial\Omega$) boundary conditions, where $q(u)$ is a polynomial function defined on $\partial\Omega$.

The standard numerical integration of the PDE is performed by the Matlab toolboxes, which are efficient for the classes of problems we deal with (see the Matlab reference books for details on these routines, e.g.[10]). We resort to the Matlab Partial Differential Equations Toolbox for the ancillary developments.

A description of the composite mesh concept is given in the next section where we define the double mesh method for error estimation.

2.1 The finite element composite mesh

The composite mesh is formed by two (or more) finite element meshes of different accuracy (different element size h), which share the problem domain. Connection between components is enforced (for instance connecting common nodes). A participation factor for each mesh is defined, for details see[4].

The main characteristics of the particular double meshes we use in this paper are:

1. Triangle element meshes
2. the finer mesh is the refinement of the coarser one obtained by subdivision of the triangles by the midpoints of the edges
3. the common nodes connect the two meshes
4. the double mesh have the sum of the elements of both, the fine and coarse meshes and the same quantity of nodes than the fine mesh
5. the participation factors are equal for the meshes
6. in the case of solution improvement the participation factors depend on the local order of the method

2.2 Error estimation

In the next section the methods for error estimation and solution improvement are stated.

In addition to the residual as estimation of errors, for some of the problems other error estimators can be considered. Among them, the Zienkiewicz-Zhu[7] and the Zadunaisky[15] methods have been tested for comparison purposes.

2.3 Mixed mesh *a posteriori* error estimator

In this section we apply the double mesh method error estimation to the border singularities problems.

2.3.1 Double mesh method

The double mesh is composed by two finite element meshes of element sizes $h_1 > h_2$. At start time the mesh is refined near the possible singular points. If these are not known in advance we resort in the method the task of locating all of them. In general the second mesh has the additional property of being a refinement of the first. The common nodes connect the two meshes so the complete set of elements are connected. The participation factor of each of the meshes is set as equal, but other arrangements are equally possible.

The ulterior application of our results to monolith catalytic reactor modeling lead us to select also the case of structured meshes of rectangular elements, where one such element shares the spatial subdomain with four elements of the finer mesh (in the case of 3D elements the subelements are eight). The nodes of the coarser element are the points of connection of the two meshes.

Other relations between the two meshes are also possible, e.g. the finer mesh should not be a refinement of the coarser. Instead a set of connection points of the domain related to both meshes could be defined and the nodal points be restricted so the connection points of the two meshes coincide.

When dealing with the case of a mesh that is a refinement of the other we form a composite of the two (with weights α and $(1-\alpha)$ respectively) so the set of their elements are the union of the elements of both and the nodes classify between common nodes and free nodes of the finer mesh. The effects of weights appear at the system of equations level. For further details of double mesh algorithm implementation see[3]

2.3.2 Error estimation

The operator problem

$$Lu = f \tag{6}$$

can be approximated —as was stated in the second section— by standard finite element method as

$$L_i u_{h_i} = f_i, \qquad i = 1, 2 \tag{7}$$

where, in general, $h_1 > h_2$, and in practical applications $h_1 = 2h_2$, h_i being the element size of finite element mesh M_{h_i}, $i = 1, 2$. The meaning of symbols h_i are the following, globally they represent the norm of the partition of the domain in elements, but locally they refer to the diameter of the element and say that the elements of size h_2 refine those of size h_1. In the usual case the meshes are connected at common nodes (they are the nodes of the coarser mesh) and one is a refinement of the other.

The mixed mesh solution $u_{h_1 h_2}$ is obtained from

$$(\alpha L_{1\to 2} + (1-\alpha)L_2)u_{h_1 h_2} = (\alpha f_{1\to 2} + (1-\alpha)f_2)$$

where the symbol $L_{1\to 2}$ stands for the immersion of matrix L_1 into the correct places of L_2 padded with zeros. The same for f.

We can define the symbol $u_{h_1 h_2 n}$ for the function, bilinear in the elements, that coincides with $u_{h_1 h_2}$ in the coarser nodes (mesh M_{h_1}) and is bilinearly interpolated in the remaining nodes (those of mesh M_{h_2} that are not on mesh M_{h_1}). And we define the symbol $u_{h_1 h_2 p}$ for the function bilinear on mesh M_{h_1} that is a projection of $u_{h_1 h_2}$ to the coarser mesh.

2.3.3 Order of the methods

As seen elsewhere[3] if $h_1 = 4h_3$ and, as before $h_1 = 2h_2$, we can write, for each common node,

$$\frac{u_{h_2} - u_{h_1}}{u_{h_3} - u_{h_2}} \simeq 2^p \tag{8}$$

expression that allows us to compute the approximate asymptotic local order of the method from the results obtained from meshes M_{h_i}, $i = 1, 2, 3$

Near the singular points in the border the order of the methods drop dramatically. The estimation of the order is then less accurate than in the parts of the domain that are far from these points. The method can detect the singular areas and refine there the mesh still in this case.

2.3.4 Improving results by extrapolation

Richardson's extrapolation, as is known, is a way to obtain an improved solution from two results corresponding to different mesh accuracy. Let M_{h_1} a finite element mesh with element size h_1 and M_{h_2} another mesh with element size h_2. Let u be the exact solution (unknown) and u_{h_i} its approximation obtained with mesh M_{h_i} ($i = 1, 2$), then

$$u = u_{h_1} + C h_1^p + O(h_1^q) \tag{9}$$

$$u = u_{h_2} + C h_2^p + O(h_2^q) \tag{10}$$

where p is the order of the approach and $q > p$. Eliminating constant C

$$u = \frac{\frac{h_1^p}{h_2^p}}{\left(\frac{h_1^p}{h_2^p} - 1\right)} u_{h_2} - \frac{1}{\left(\frac{h_1^p}{h_2^p} - 1\right)} u_{h_1} + O((\max\{h_1, h_2\})^q) \tag{11}$$

and if $h_1 = 2h_2 = 4h_3$

$$u_{h_1 h_2 r} = \frac{2^p}{(2^p - 1)} u_{h_2} - \frac{1}{(2^p - 1)} u_{h_1} \tag{12}$$

$u_{h_1 h_2 r}$ in 12 is the Richardson's extrapolation between meshes M_{h_1} and M_{h_2}. This solution is computed over the nodes of the coarse mesh (M_{h_1}).

If a third mesh M_{h_3} is defined as a refinement of M_{h_2} then

$$\frac{u_{h_2} - u_{h_1}}{u_{h_3} - u_{h_2}} \simeq \frac{{h_1}^p - {h_2}^p}{{h_2}^p - {h_3}^p} \tag{13}$$

and if $h_1 = 2h_2 = 4h_3$

$$\frac{u_{h_2} - u_{h_1}}{u_{h_3} - u_{h_2}} \simeq 2^p \tag{14}$$

This expression allows us to compute the approximate order of the numerical method, from the results of three meshes M_{h_1}, M_{h_2} and M_{h_3}.

2.3.5 Estimation of errors via extrapolation

We have just obtained the extrapolation formula

$$u_{h_1 h_2 r} = u_{h_2} + \frac{1}{2^p - 1}(u_{h_2} - u_{h_1}) \tag{15}$$

the symbol $()_r$ stands for Richardson extrapolation.

In equation 15 the term $\frac{1}{2^p-1}(u_{h_2} - u_{h_1})$ can be interpreted as the principal part of the extrapolation correction. In the case of $p = 2$ the coefficient is $1/3$, tending to 1 when the order degrades towards one.

The local order obtained from equation 8 is needed in equation 15 for the extrapolation. Their are also useful for the determination of weights in the extrapolation-like double mesh method for solution improvement.

The meaning of the Richardson correction is that, in each node common to the two meshes is necessary to add to the nodal value u_{h_2} the error estimation so the value $u_{h_1h_2r}$ be a step nearer the true value u (the next order in the asymptotic error expansion). In the points of the second mesh that are not common with those of the first one we can calculate a bilinear interpolant. The symbol $u_{h_1h_2rn}$ represents the interpolated values from the Richardson extrapolation, and the symbol $u_{h_1h_2rp}$ the projected values to the coarser mesh that coincide with $u_{h_1h_2r}$. For example, if $h_1 = 1/20$ and $h_2 = 1/40$, the bilinear functions u_{h_2}, $u_{h_1h_2}$, u_{h_1n}, $u_{h_1h_2pn}$ $u_{h_1h_2rn}$, are all of size 41×41, and u_{h_1}, $u_{h_1h_2p}$, u_{h_2p}, $u_{h_1h_2r}$, $u_{h_1h_2rp}$, are all of size 21×21.

2.3.6 Residuals

We can calculate the following residuals

$$r_i = L_i u_{h_1h_2} - f_i \tag{16}$$

the solution $u_{h_1h_2}$ being adapted to the dimension of the matrices involved.

We can prove that

$$r_1 + r_2 = 0 \tag{17}$$

over the nodes.

The double mesh solution $u_{h_1h_2}$ lies, in general terms, between the solutions u_{h_i}, $i = 1, 2$. So the sum of the absolute values of the residuals is related and in a direct proportion to the difference between the two approximate solutions and to their absolute errors. The main idea is that the estimation can be done with only one double mesh calculation.

2.3.7 Band integrals of the residuals

In some of the applications the constructed rectangular grids (double meshes) of size $h = h_1$ were obtained from simple rectangular finite element meshes of size h, e.g. in the case of catalytic reactors it is advisable to construct a mesh that is refined near the catalyzer and so the bands are less coarse there than in the bulk channel. Each element of a finite element mesh (in 2D) is subdivided into four rectangular components of size $h/2 = h_2$. We then obtain a new simple finite element mesh of general size $h/2$. In a rectangular double mesh of size h, each element of the simple coarse mesh shares the same domain with four elements of the finer mesh, their common nodes being those of the coarser one.

The j band integral of the residuals is

$$R_j = \sum_{i=1,2} \sum_{e_i^j} \sum_{p_i(e_i^j)} \omega_{p_i(e_i^j)} r_i^2(p_i(e_i^j)) \tag{18}$$

where e_i^j stands for the index of elements of the meshes ($i = 1$ for the coarser, $i = 2$ for the finer) in the band j considered. The symbols $p_i(e_i^j)$ and $\omega_{p_i(e_i^j)}$ are the integration nodes and weights for the element e_i^j.

3 BOUNDS FOR THE RESIDUALS

By Céa's lemma (at least for the linear cases) there exists a constant C such that

$$\|e_2\| = \|u - u_{h_2}\| \leq C\|u - u_{h_1h_2}\| \tag{19}$$

and, of course

$$\|e_1\| = \|u - u_{h_1}\| \leq C_3\|u - u_{h_1h_2}\| \tag{20}$$

also, in general, there exists a constant C_2 such that

$$\|u - u_{h_1h_2}\| \leq C_2\|u - u_{h_2}\| \tag{21}$$

so there exist constants D, $\tilde{C}$ such that

$$\|r_2\| \leq D\|u_{h_2} - u_{h_1h_2}\| \leq \tilde{C}\|u - u_{h_2}\| = \tilde{C}\|e_2\| \tag{22}$$

this inequality guarantees the relation between the residuals and the errors in the sense that if the real errors are low the residuals must rest accordingly low.

The other inequality, needed for the normed equivalence between these measures of error, with constant $\tilde{C}_2$,

$$\|e_2\| = \|u - u_{h_2}\| \leq \tilde{C}_2\|r_2\| \tag{23}$$

is also necessary and we have obtained this in particular cases. The main problem is: a general proof is still lacking, we are confident to solve this problem in the following and show the results soon. Obtained this the equivalence between residuals and errors is complete. Of course these equivalence is useful in a local framework in our construction:

These inequalities are also valid in a local framework: it is necessary to center in a concrete element and take the nearest neighbor elements region. There the same inequalities can be proved (we are working on the last one). These local bounds allow to justify the adaptive procedure based on the residuals (local integration of the residuals like the band integration of previous subsection).

4 ELLIPTIC TEST PROBLEMS REVISITED

In[4] and several recent *Enief* and *Mecom* presentations we have treated several elliptic test examples in order to assess the quality of element residuals as *a posteriori* error estimators. A representative sample of these is shown here for the sake of completeness.

The first examples are the double mesh solution of Laplace equation with Dirichlet boundary conditions and a retract angle singularity.

A family of Laplace problems with singularities were studied over the unit square. Here the solutions are

$$u(x,y) = ((x-\frac{1}{2})^2 + (y-\frac{1}{2})^2)^{\frac{\pi}{2\omega}} \cos\frac{\pi}{\omega}\theta, \qquad \theta = \arctan((y-\frac{1}{2})/(x-\frac{1}{2})) \tag{24}$$

$\omega = 2\pi - 2\beta$, and several values for angle of aperture 2β. For example the case $\beta = \arctan(\frac{1}{1000})$ is treated. The order of the singularity is associated with β. If a solution improvement is to be performed (see[3] the participation factor α depends on the order of singularity.

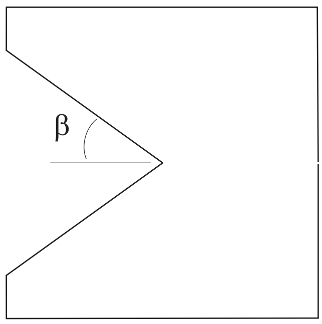

Figure 1: Domain contained in the unit square, example 1.

Fig. 1 shows the domain of this family of examples: a unit square without a centered angle of various apertures, from near zero (approximated crack) to a value that is greater than π.) In this case the aperture of the retract angle lead to a vertex that is a singular point in the boundary of the domain. On the boundaries the border conditions are Dirichlet.

In the next subsections we show brief quotations of our previous study of several cases for aperture angle 2β and the order of the methods from the norms of errors for the meshes of different granulometry.

4.1 Angle $\pi/2$

In the Table 1 we show the fine mesh errors (exact errors from exact solution) for the angle $2\beta = \pi/2$ case. There u is the exact solution and u_h is the (simple) finite element solution for the fine mesh. We consider the energy, L_2, and sup norms for different quantity of nodes in the mesh. In the L_2 norm case it is possible to observe the superlinear order that corresponds to this aperture. In this case the theoretical order is $3/2$ so our results are coincident with the theoretical order expected.

Table 1: Fine mesh errors (exact errors), angle $\pi/2$.

Nodes	$\|u-u_h\|_E$	$\|u-u_h\|_{L_2}$	$\|u-u_h\|_{L_\infty}$
142	$3.2e{-}4$	$3.24e{-}3$	$1.1e{-}2$
519	$1.3e{-}4$	$1.3e{-}3$	$7.3e{-}3$
1981	$5.45e{-}5$	$5.1e{-}4$	$4.7e{-}3$
5025		$2.01e{-}4$	$3.0e{-}3$

Observation: In the L_2 norm column we observe the superlinear order.

4.2 Very little angle: crack

The residuals, the Zienkiewicz-Zhu error estimators and the Zadunaisky's method error estimator have similar patterns and all detect the corner singularity.

In the Table 2 we show the previously obtained fine mesh errors (also exact errors) for the domain with an angle near zero (crack) in order to estimate the order of the method.

The energy, L_2 and sup norms are included in function of the quantity of nodes in each mesh. In the L_2 norm column we observe the lineal order. In this case the theoretical order is near 1

Table 2: Fine mesh exact errors for the crack domain.

Nodes	$\|u-u_h\|_E$	$\|u-u_h\|_{L_2}$	$\|u-u_h\|_{L_\infty}$
97	$6.6e{-}3$	$1.63e{-}2$	$4.27e{-}2$
345	$3.6e{-}3$	$8.02e{-}3$	$3.47e{-}2$
1297	$1.9e{-}3$	$3.96e{-}3$	$2.61e{-}2$
5025		$1.97e{-}3$	$1.9e{-}2$

Observation: In the L_2 norm column appears the lineal order of the method.

When comparing the residuals computed with the double mesh and exact errors, we have observed that the residuals are able to detect the singular point in the boundary of the domain. The objective of the computation of the residuals is to detect the elements with the bigger errors. In this case those near the singular point.

The sup norm of residuals is bounded in this case for those of the exact errors.

4.3 Angle near π, non convex case

The precedent cases are the classical ones in the verification of a method adapted to local error detection. We also show previous results for the cases of convex and non convex polygonal domain with angle near π. These cases are important because the theoretical order is near 2 but the residuals are still efficient for the detection of the singular node (center of the unit square).

We have an uniform improvement in the solutions due to the fact that the singularity is much lesser demandant. See the respective tables with the errors.

In the first place we recall the non convex case and then the convex one

In Table 3 we show the double mesh errors with respect to the exact solution for the domain with an angle of $\pi - \varepsilon$ (non convex case) The same norms than in the precedent cases are included. And in the L_2 norm column we observe the order near 2. In this case the participation factor for solution improvement results should be of approximately $\alpha = 4/3$

Table 3: Double mesh errors (exact errors) for the domain with angle $\pi - \varepsilon$ (non convex case).

Nodes	$\|u - u_{h_1 h_2}\|_E$	$\|u - u_{h_1 h_2}\|_{L_2}$	$\|u - u_{h_1 h_2}\|_{L_\infty}$
373	$4.8e{-}11$	$4.2e{-}7$	$3.2e{-}6$
1417	$1.1e{-}11$	$1.2e{-}7$	$1.6e{-}6$
5521	$2.7e{-}12$	$3.5e{-}8$	$8.2e{-}7$

Observation: See the quadratic order in the L_2 column.

4.4 Angle near π, convex case

In this case, that is complementary of the precedent, the domain is nearly a rectangle with an angle slightly greater than π with vertex in the center of the unit square. It is indeed a convex polygon but in this case we also detect the singularity in the vertex and its consequences.

Here the solution of the problem resides in the H^2 space and the previous ones in the space H^{1+s}, con $0 < s < 1$.

In the Table 4 we show the double mesh exact errors in the same norms than before. Here the order is 2

The sup norm of residuals and exact errors are very similar.

In Fig 2 we plot the solution of the test problem with the mesh superimposed and the error plotted in darker shade.

4.5 Orders of methods

In the figure 3 we plot the sup and L_2 norms for different meshes. We obtain the orders from the slope of the curves: in the L_2 norm case for the crack example the order is linear; in the L_2 norm case for the angle $\pi/2$ example the order is superlinear (near $5/3$). The sup norms show lower orders of convergence.

Table 4: Double mesh exact errors for the angle $\pi + \varepsilon$ (convex case).

Nodes	$\|u - u_{h_1h_2}\|_E$	$\|u - u_{h_1h_2}\|_{L_2}$	$\|u - u_{h_1h_2}\|_{L_\infty}$
371	$4.4e{-11}$	$4.4e{-7}$	$3.1e{-6}$
1413	$1.0e{-11}$	$1.3e{-7}$	$1.4e{-6}$
5513	$2.5e{-12}$	$3.7e{-8}$	$7.4e{-7}$

Observation: Quadratic order.

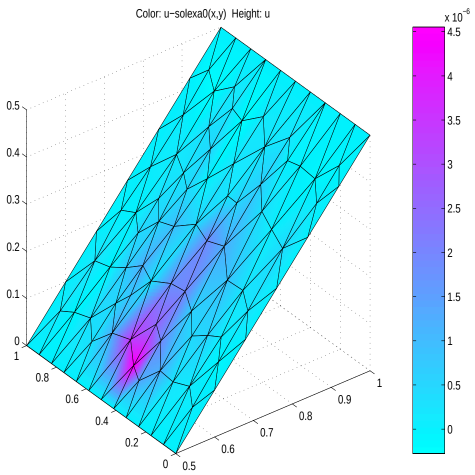

Figure 2: Test problem. Angle near π (convex case). The mesh is superimposed and the errors are concentrated near the vertex. Note that it is a convex polygonal domain.

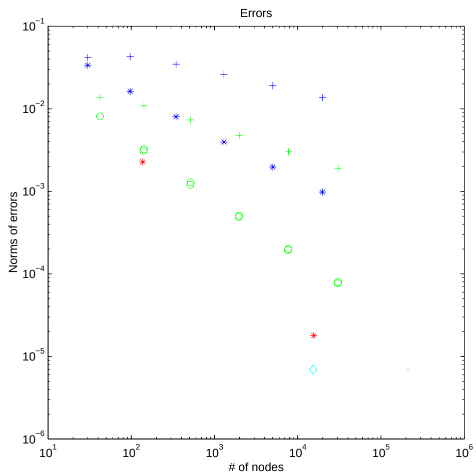

Figure 3: Error norms: $+$(blue): sup norm (crack), $*$(blue): L_2 norm (crack), $+$(green): sup norm (a. $\pi/2$), o(green): L_2 norm (a. $\pi/2$), $*$(red): L_2 norm (crack) adapted mesh.

5 NONLINEAR AND ADVECTIVE PROBLEMS

In this section we treat elliptic stationary examples associated with advective and nonlinear terms.

The methodology proposed is able to perform error estimation in a set of more complex problems than those of this section. The main characteristics are: (1) systems of equations, (2) advective terms, and (3) nonlinear coefficients.

Also in this section several problems associated to the modeling of catalytic chemical reactors are considered.

5.1 Example 2

In this example we recall a non advective non linear elliptic equation associated to a parabolic equation with known exact solution that reads

$$-\Delta u + (1+u)u = (1+x^2+y^2)(x^2+y^2) - 4, \qquad \text{in } \Omega = [0,1]^2 \tag{25}$$

with the boundary conditions $\frac{\partial u}{\partial \eta}(0, y) = 0$, $0 \le y \le 1$, $x = 0$; $\frac{\partial u}{\partial \eta}(x, 0) = 0$, $0 \le x \le 1$, $y = 0$; $u(1, y) = (1 + y^2)$, $0 \le y \le 1$, $x = 1$; $u(x, 1) = (1 + x^2)$, $0 \le x \le 1$, $y = 1$; so the exact solution of this test problem is $u(x, y) = (x^2 + y^2)$.

This equation is of the same type of models of temperature diffusion in a 2D chemical reactor with Neumann and Dirichlet boundary condition. The residuals detect the change (gradients) in the errors of the methods.

The next example includes nonlinear and advective terms.

5.2 Example 3

In this example the nonlinearities appear in the main body of the equation, an advective term represents the flux of matter inside the 2D reactor and nonlinear (polynomial) boundary conditions represent the catalytic chemical reaction on the top wall of the reactor. The equation is

$$-\Delta u + (1 + u)u + 2(1 - y)^2 \frac{\partial u}{\partial x} = 0, \qquad \text{in } \Omega = [0, 1]^2 \tag{26}$$

with the boundary conditions $u(0, y) = 1$, $0 \le y \le 1$, $x = 0$; $\frac{\partial u}{\partial \eta}(x, 0) = 0$, $0 \le x \le 1$, $y = 0$; $\frac{\partial u}{\partial \eta}(1, y) = 0$, $0 \le y \le 1$, $x = 1$; $\frac{\partial u}{\partial \eta}(x, 1) = -u^2$, $0 \le x \le 1$, $y = 1$;

Based on the residuals corresponding to double mesh ($\alpha = 0.5$) solutions we refine adaptively the meshes. Here the exact solution is not known so the reference must be done versus a finer mesh finite element solution. In this case the residuals also detect the zones with greater errors.

5.3 Example 4: systems of elliptic equations

This subsection follows the companion paper[11] and is included for the sake of completeness.

Monolith catalytic reactors can be modelled by systems of partial differential equations. These equations represent the mass and energy balances inside the reactor. The complete and detailed system is so complex that several simplifications are in order for a mathematical study of the principal characteristics and properties of the original system.

The first simplifications (they are not essential but very convenient) lead to a system in two spatial dimensions (radial symmetric submodels) and only one species to be treated, so we have two equations one for the mass balance of this species and the other for the heat balance of the reactor.

The first steps in the mathematical analysis of the problem are towards the study of the equations in a non coupled form. For them we perform determination of the ranges for the approximated solutions and study characteristics of the solutions, if they are monotonic, range of values of operation, etc. The goal is to consider the possibilities in the case of coupling of the equations.

In the domain where the problem is studied the catalytic substance is on one of the walls of the catalytic tube, in this case the upper wall (see Fig. 4). Here the main chemical reaction takes

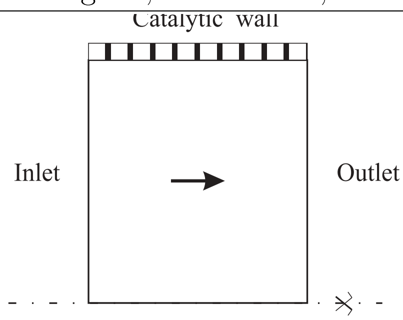

Figure 4: Schematics of the catalytic reactor domain.

place. The heat transfer processes also are concentrated in this wall. The other portions of the boundary of the domain are the inlet where the values of the temperature and concentration are known, and the other two sides of the unit square where Neumann conditions are imposed.

The length of the reactor is variable. In our examples we take the adimensional unitary distance for the sake of simplicity. The longer the reactor, the greater the amount of elimination reaction of the target species. The mean length of the reactor can be used as a design parameter.

The simplified equation that models the process: concentration w of a chemical species (e.g. propane) in a oxygen rich atmosphere is

$$-\Delta w + auw = 0 \tag{27}$$

where a is a parameter and u is the temperature of the domain (we take the unit square)

The boundary condition on the catalytic boundary are

$$\partial w/\partial \eta + buw = 0 \tag{28}$$

where the symbol $\partial w/\partial \eta$ corresponds to the normal derivative of w and b is a parameter. The other boundary conditions are standard as was explained.

The simplified equation for the distribution of temperatures in our domain is

$$-\Delta u + cwu = 0 \tag{29}$$

where c is a parameter.

The Robin boundary conditions on the catalytic boundary are

$$\partial u/\partial \eta - dwu = -f(u) \tag{30}$$

where d es a parameter and $f(u)$ is a function of temperature u (heat transfer processes)

In order to solve this problem we use an iterative method. We start with a concentration distribution provided by the uncoupled equation. Then the heat equation is solved and the residuals are studied in order to decide if the mesh has to be refined (near the singular vertex) so we obtain a new temperature distribution. The equation of concentrations is then solved (under the new temperature distribution) and the residuals are calculated.

The new distributions are compared to the previous two and the process continues till an acceptable level of tolerance.

After convergence in concentrations and temperatures, in Fig. 5 the residuals corresponding to the concentrations are shown. See that the residual map detects the singularity (due to the unmatching of the boundary conditions)

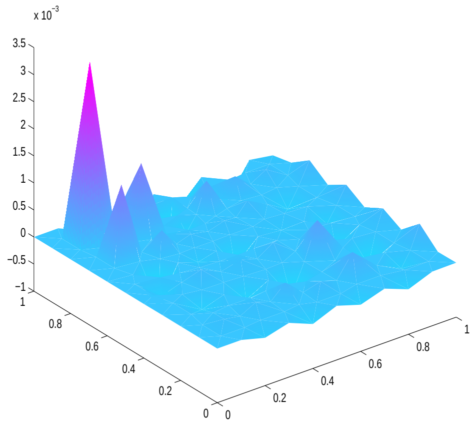

Figure 5: Residuals corresponding to the concentrations.

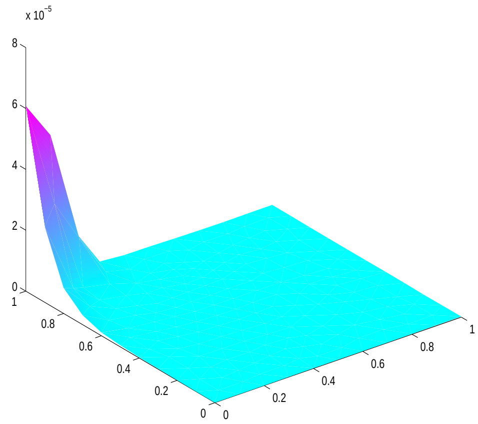

Figure 6: Zienkiewicz-Zhu errors for concentrations distribution.

In the Fig. 6 we show the Zienkiewicz-Zhu error estimation for the same estimation as Fig. 5 It is possible to see the general agreement of both estimations.

6 LINEAR ELASTICITY EXAMPLE

6.1 Singularities in a structural problem: cracked strip

The double mesh method has been applied to a problem of interest in structural mechanics, which is the stress concentration around the tip of crack. For this, a plane stress problem of a strip subject to a uniform tension load and with a crack transverse to the load direction has been studied.

The case to be analyzed is shown in figure 7. A linear elastic analysis have been performed. Due to the symmetry a half domain has been modelled.

The deformed mesh computed with a standard finite element mesh is shown in figure 8, and the map of principal tension stress in figure 9. The stress concentration around the crack tip may be seen in this figure.

The double mesh with $\alpha = 0.5$ has been used in order to estimate the errors. The residuals obtained are drawn in figure 10. It may be observed that errors are also concentrated in the region around the crack tip.

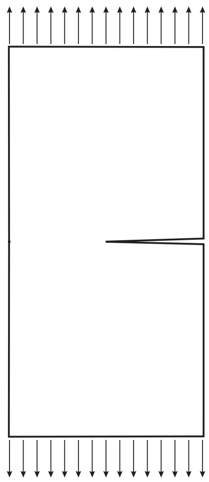

Figure 7: Problem of a tensed cracked strip.

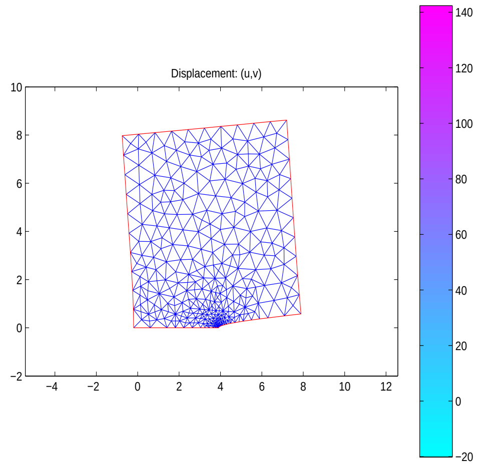

Figure 8: Crack problem: deformed mesh.

7 IMPROVING FINITE ELEMENT SOLUTIONS WITH A MIXED MESH

In the previous sections some results have been shown where the double mesh is used in order to obtain error estimations of the numerical solution. The double mesh may also be used in order to obtain improved solutions. In this case the participation factor is selected as $\alpha > 1$ leading to a sort of extrapolated behavior of the Finite Element model. Some results either for regular or singular problems are shown in the following.

7.1 Elliptic problem with a retract angle

The example 1, of a square domain with a retract angle $2\beta = \frac{\pi}{2}$, has been modelled with double mesh with a participation factor $\alpha = \frac{5}{3}$.

The L_2 norm of the error for a mesh with 519 nodes is $7.2e-4$ and for 1981 nodes is $2.3e-4$. These values should be compared with those in the L_2 column of Table 1. The exact errors for the double mesh with $\alpha = \frac{5}{3}$ are roughly $\frac{1}{2}$ the exact errors for the fine mesh. These results are for a problem with singularities, and it should be pointed out that the computational effort is roughly the same for the double and the fine mesh. The optimal value for the the participation factor in this case is $\alpha = 1.46$.

7.2 Elastic problem

An elastic cantilever beam has been studied as 2D plane stress problem in reference[13]. Using a double mesh with $\alpha = \frac{4}{3}$ accurate results has been obtained. Figure 11 shows the global relative error in L_2 norm vs. the number of unknowns, for: the simple mesh; the composite mesh with $\alpha = \frac{1}{2}$; and the composite mesh with $\alpha = \frac{4}{3}$. The effect of the extrapolation implied in the double mesh strategy is clear in this figure. The displacement of the beam tip is shown in figure 12 for which the comments are the same as for figure 11.

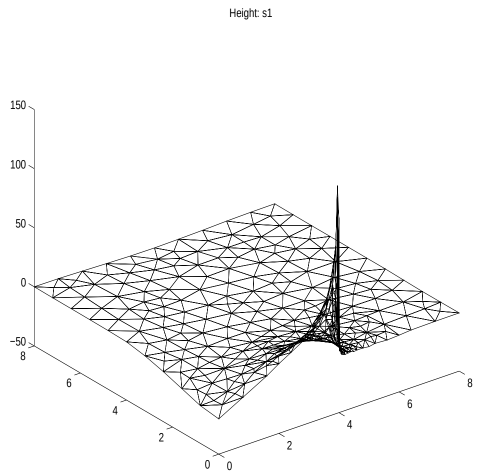

Figure 9: Crack problem: map of principal stress.

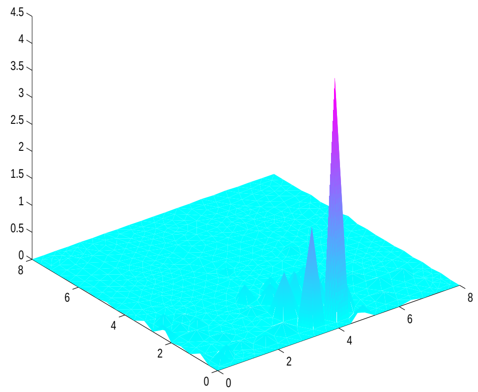

Figure 10: Crack problem: residuals.

7.3 Elastic problem with singularity

The problem of a cracked strip, shown in figure 7, has been studied with a composite mesh using $\alpha = \frac{4}{3}$ (see[3]). Figure 13 shows the global relative error in infinity norm of the displacement vector for: the simple mesh; the composite mesh with $\alpha = \frac{1}{2}$; and the composite mesh with $\alpha = \frac{4}{3}$. The comments are similar as for the previous example.

8 CONCLUSIONS

The use of a composite, or mixed, finite element mesh for elliptic problems with border singularities is studied. Two or more finite element meshes are allowed to share the problem domain. These component meshes have different intrinsic accuracies and are affected each by a weight or participation factor. The composite mesh has been used to estimate *a posteriori* discretization errors.

A semiquantitative error estimator based in a double mesh algorithm has been proposed and we have shown that the pattern of this *a posteriori* error is similar to the exact error.

More research is still needed, but the composite mesh method appears to be a powerful and simple tool for obtaining accurate finite element error estimation and allow for adaptivity of meshes.

It is interesting to note that, including convex polygonal domains, the error estimator is efficient and it is not related to the order of the method.

When the singularities are created by the non conforming boundary conditions in a vertex of the polygonal domain the method is also efficient even in case of nonlinear methods.

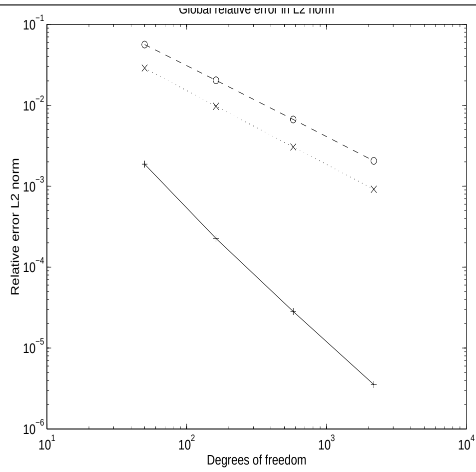

Figure 11: Cantilever beam problem: Global relative error in L_2 norm (x) Simple mesh; (o) Composite mesh $\alpha = \frac{1}{2}$; (+) Composite mesh $\alpha = \frac{4}{3}$

REFERENCES

[1] V.E. Sonzogni, M.B. Bergallo and C.E. Neuman, “Uso de una malla compuesta para estimar errores de discretización y mejorar la solución en elementos finitos” *Proceedings MECOM’96* (Tucumán, Sep’96) **I**, 123–132, (1996).

[2] M. B. Bergallo, C. E. Neuman and V. E. Sonzogni, “A finite element error estimation based on the mixed mesh concept”, *Proceedings WCCM’98* (Buenos Aires, Jul’98) (1998).

[3] V.E. Sonzogni, M.B. Bergallo and C.E. Neuman, “Improving a finite element solution by means of a composite mesh”, *Proceedings WCCM’98* (Buenos Aires, Jul’98) (1998).

[4] Bergallo, M.B., Neuman, C.E., y Sonzogni, V.E., “Composite mesh concept based FEM error estimation and solution improvement”, *Computer methods in applied mechanics and engineering*, **188**, 755–774, (2000).

[5] C. Truesdell and R. Toupin, *The classical field theories*, Ed. by S. Flugge, Handbuch der Physik II/I, Springer Verlag, Berlin, (1960).

[6] A.C. Green and P.M. Naghdi, “A dynamical theory of interacting continua”, *International Journal of Engineering Science*, **3**, pp. 231-241, (1965).

[7] O.C. Zienkiewicz and J.Z. Zhu, “A simple error estimator and adaptive procedure for practical engineering analysis”, *International Journal on Numerical Methods in Engineering* **24**, 337–357, (1987).

[8] J.R. Stewart and Th.J.R. Hughes, “A tutorial in elementary finite element error analysis: A systematic presentation of *a priori* and *a posteriori* estimates”, *Computer Methods in Applied Mechanics and Engineering* **158**(1/2), 1–22, (1998).

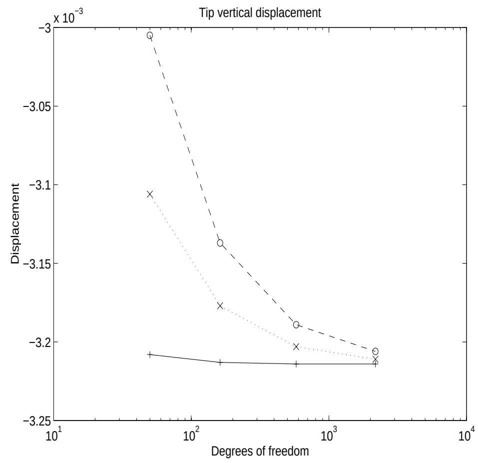

Figure 12: Cantilever beam problem: Vertical displacement of the beam tip (x) Simple mesh; (o) Composite mesh $\alpha = \frac{1}{2}$; (+) Composite mesh $\alpha = \frac{4}{3}$

[9] R. Verfürt, *A Review of A Posteriori Error Estimation and Adaptive Mesh-Refinement Techniques*, Wiley–Teubner, Chichester, (1996).

[10] L. F. Shampine, and M. W. Reichelt, *The Matlab ODE Suite*, The Mathworks, Natick, MA, 1–22, (1997).

[11] C.E.Neuman, “Modeling of catalytic reactors as elliptic problems with essential border singularities”, MECOM2004 (Bariloche, November 2004)

[12] M.B. Bergallo and C.E. Neuman, “Polynomial Finite Element Models of Monolith Catalytic Converters”, *Proceedings RPIC’97* (San Juan, Sep’97) **I**, 313–318, (1997).

[13] V. E. Sonzogni and M. B. Bergallo, “Towards a Mixture Theory type of Error Estimators for Finite Elements”, in: M. Rysz, L.A. Godoy and L.E. Suarez, eds., *Applied Mechanics in the Americas* The University of Iowa **5**, 260–263, (1996).

[14] O.C. Zienkiewicz and J.Z. Zhu, “Adaptativity and mesh generation”, *International Journal on Numerical Methods in Engineering* **32**, 783–810, (1991).

[15] Zadunaisky, P.E., “On the Estimation of Errors Propagated in the Numerical Integration of Ordinary Differential Equations”, *Numerische Mathematik*, **27**, 21–39, (1976).

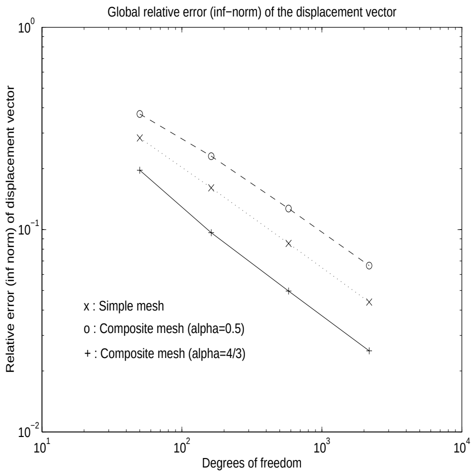

Figure 13: Crack problem: Global relative error in infinity norm of the displacement vector (x) Simple mesh; (o) Composite mesh $\alpha = \frac{1}{2}$; (+) Composite mesh $\alpha = \frac{4}{3}$